

# LWD AZIMUTHAL DENSITY LOGGING IN LIVERPOOL BAY, UK AS AN AID TO COMPLETION PLANNING VIA FAULT AND FRACTURE DETECTION

Giancarlo Rizzi and Brian Callaghan  
Jonathan Lean, David Lawton and Alison Clarke  
Tim Parker

Copyright 2007, held jointly by the Society of Petrophysicists and Well Log Analysts (SPWLA) and the submitting authors.

This paper was prepared for presentation at the SPWLA 48<sup>th</sup> Annual Logging Symposium held in Austin, Texas, United States, June 3-6, 2007.

## ABSTRACT

A logging while drilling (LWD) Azimuthal LithoDensity (ALD) imaging tool was run in horizontal dual lateral wells 110/15-L13 and 110/15-L13z with the aim of identifying fault and fracture intersections. The wells are located in the BHPBilliton operated Lennox Field, in the Liverpool Bay area of the East Irish Sea Basin, United Kingdom Continental Shelf (UKCS).

Image quality is good and numerous geological features have been identified. Fractures have been classified as either high density or low density, relative to host formation. A total of 184 fractures have been identified in L13 while 121 fractures were identified in L13z. When corrected for borehole bias, 529 fractures are calculated to intersect L13 while 241 fractures are calculated to intersect L13z. Fracture orientations are consistent with the strike of regional scale faults. Fractures in L13 and L13z strike north-south, with minor north-northwest to south-southeast components.

Significant drilling mud losses in the vicinity of fractures suggest that some fractures were open and therefore acted as fluid escape conduits. Drilling mud seepages within intervals that contain no apparent fractures may be related to fracture cuts that are below the resolution of the ALD sensor. It is also possible that some fractures became dilated after passage of the LWD tool assembly.

Real time utilization of the LWD and ALD data enabled the operator to plan and locate External Casing Packers (ECPs) and the completion string quickly and accurately, thus removing conventional logging delays (and costs) while the drilling rig was on location.

## INTRODUCTION AND GEOLOGICAL CONTEXT

The Lennox Field is located in UK blocks 110/14a and 110/15a, in the Liverpool Bay area of the East Irish Sea Basin (Figure 1). The structure comprises a faulted roll over anticline which is located along the hanging wall of the Formby Point Fault. The reservoir consists of Triassic Ormskirk Sandstone Formation, part of the Sherwood Sandstone Group (Jackson and Mulholland 1993; Jackson and Johnson 1996; Warrington *et al.*, 1999). This comprises a series of aeolian and fluvial dominated sandstones (Meadows and Beach 1993; Meadows, 2005, 2006; Thompson and Meadows, 1995, Macchi, 2000). These are fractured and faulted on the eastern side of the field. Porosity ranges from 11-21% with air permeabilities of between 50 md and 10 darcies. The Ormskirk reservoir is subdivided into four vertically stacked reservoir zones which have contrasting petrophysical properties, a reflection of their contrasting depositional textures and compositions (Yaloz *et al.*, 2002; Yaloz and Chapman, 2003). Zones I, II and III intersect the oil rim and gas cap, whilst Zone IV is in the aquifer. Zones I and III consist predominantly of excellent quality aeolian dune and sandsheet lithofacies. Zones II and IV consists of moderate reservoir quality fluvial sandstones.

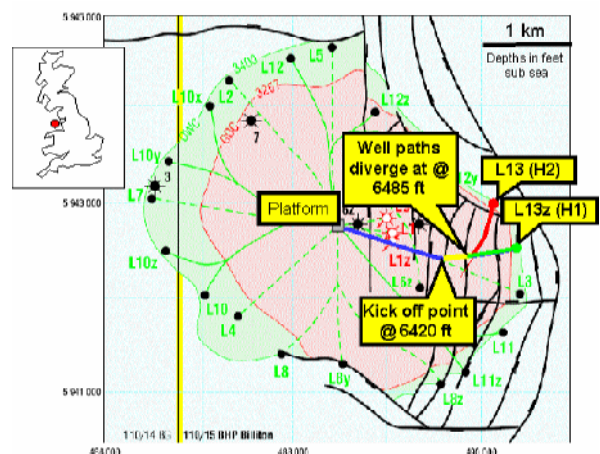
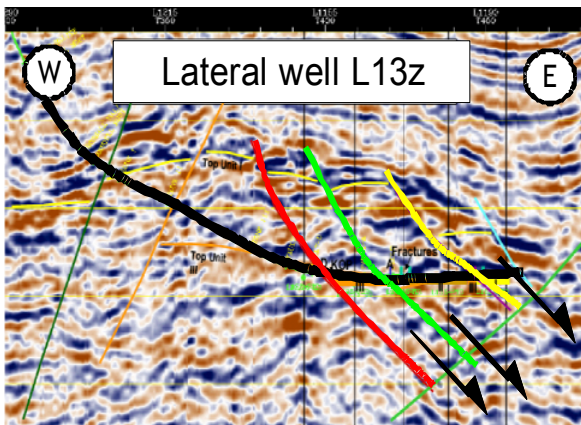


Figure 1: Top structure map of the Lennox Field showing the L13 and L13z well paths. The wells were drilled in the eastern

part of the field as a side track to the poorly performing L3 well. Yellow line segment indicates shared L13 and L13z well path trajectory. Inset map shows location of Liverpool Bay Development (red dot).

In the eastern part of the field, three seismic scale faults denoted Fault D (red), Fault A (green), and Fault B (yellow) have down faulted reservoir zones to the northeast (Figure 2). This down faulting has produced a complex repeat stratigraphy along the L13 and L13z well paths (Table 1).

The field was discovered in 1992 and then appraised by three further wells. Development drilling has been phased since project sanction was granted in 1993. The field has been developed with long horizontal and multilateral wells placed low in the 143ft oil rim to minimize coning from the gas cap and water leg. The L13 dual lateral well was drilled in the summer of 2005 and is the latest in a series of staggered drilling campaigns to maximise Lennox oil production.



**Figure 2:** Seismic section with superimposed L13z lateral well path (black line) showing the location of major prognosed fault cuts. Fault D (red), Fault A (green), and Fault B (yellow). The L13 well path show the same faults location and has not been shown for reasons of clarity.

Oil production commenced from the field in 1996 with plateau oil production rates of 40,000 stb/d. Guidelines have been in place since the start of production to minimise drawdown. This has maximized recovery from the oil leg by keeping movement of the gas-oil and oil-water contacts to a minimum. All produced gas from the field (until August 2003), has been re-injected to maintain reservoir pressure. The production characteristics of the field are in the process of a fundamental change as the field transforms from oil to gas production. Gas from the Liverpool Bay Development (including Lennox gas cap gas) is contracted at current peak rates until 2007. With the adjacent Liverpool Bay gas fields in decline, Lennox gas is now split into sales gas and injection gas.

Accordingly, reservoir pressure is falling. The latest Lennox Field development campaign was aimed at increasing oil production from the field in the time remaining before full gas cap blowdown.

Lateral well	Interval (mD)	Zone	Ormskirk Sandstone Formation member
L13	5875-7040 ft	III	1
	7040-7408 ft	II	2a
	7408-8215 ft	III	1
	8215-9125 ft	II	2a
L13Z	6420-7181 ft	III	1
	7181-8118 ft	II	2a
	8118-8270 ft	III	1
	8270-8735 ft	I	2b

**Table 1:** Repeat stratigraphy and reservoir zones encountered by lateral wells L13 and L13Z well paths as a result of down faulting towards the east. Red dashed line = fractured contact. Blue dashed line = fractured / faulted contact. Note fractures typically occur at reservoir zone boundaries.

**L13 HISTORICAL PERSPECTIVE**

A useful historical perspective of the L13 drilling campaign is provided by Clarke *et al.* (2006). Lennox oil had recently come off plateau rates when sales gas was required from the reservoir in late 2003. Gas re-injection rates were reduced causing a fall in reservoir pressure. Wells with water cutting then began to have severe lift problems; this imposed blowdown had started to impact oil production and hence reserves.

With reservoir pressure falling with production and increasing lift problems (and high oil prices), a review of remaining Lennox Field opportunities was undertaken. Two areas were thought to contain unswept oil; an area directly beneath the Lennox platform, and an area in the eastern part of the field. The area beneath the Lennox platform was thought to be unswept because previous wells were drilled radially from the platform and did not intersect underlying formations. The eastern area was prognosed unswept due to insufficient time allowed for well L12 (drilled in December 2002) to drain the area and the poor production performance of the L3 single well bore.

A number of simulation model predictions were made to test the viability of a new development well. These models indicated the area to the east was most attractive in terms of potential recoverable volumes. For these reasons, a proposal was made to drill horizontal well L13 as a side track to the poorly performing L3 well. Well L3 was drilled early in the field development but suffered from fracture and fault zone intersections. Although the major fault zones were isolated with ECPs, this was done for logging purposes only and not

all of the fracture zones were isolated. The early performance of the well was dominated by water production and water loading, preventing oil from flowing. The well was shut-in for a number of years before being brought back on-line using coiled tubing and nitrogen to unload water from the wellbore. The well came back on at initially high oil rates, but this declined rapidly as gas entered the well and gas-oil-ratio (GOR) increased. Fractures intersected by the well, which were not isolated during the initial completion, provided a conduit for water to rise from the underlying aquifer. The well died as water collected in sumps along the wellbore. Later in field life, when reservoir pressure had started to fall and downward movement of the gas-oil-contact had commenced, fractures provided a path for gas from the gas cap to enter the wellbore, greatly increasing the GOR of the well.

The loss of L3 due to fracture and fault induced water breakthrough, dictated that the L13 well would have to be logged carefully so that faults, fracture zones and individual fractures could be identified and subsequently isolated, thus preventing a recurrence of the poor performance observed in the well L3. The tool chosen to achieve this was the Azimuthal LithoDensity (ALD) imager.

**AZIMUTHAL LITHO-DENSITY TOOL**

Compared to conventional borehole imaging tools, the logging while drilling Azimuthal LithoDensity tool acquires relatively low resolution images. However, using a sound knowledge of structural geology and borehole geometric relationships, it is entirely possible to generate rigorous azimuthal (north referenced) spatial data. The ALD tool comprises a supply of Caesium<sup>137</sup> and pair of near and far detectors which are housed within a drilling stabilizer (Figure 3). Caesium<sup>137</sup> acts as a source of gamma ray emissions.

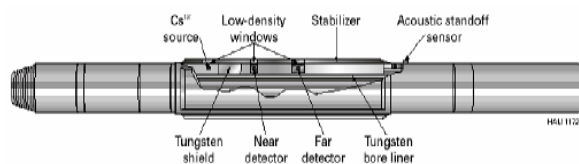


**Figure 3:** The Azimuthal LithoDensity (ALD) tool assembly. Length of tool is circa 15 ft.

The count-rates from the detectors are sampled every 20 milliseconds, with each sample being assigned to one of 16 azimuthal bins. Each bin is orientated using information supplied from tool magnetometers. The 20 millisecond samples accumulate in each azimuthal bin over a predetermined period, typically around 16 seconds. At the end of this period, the accumulated

samples are summed together and used to calculate a density for each bin. Formation density is related proportionally to the number of returned emissions of gamma radiation. Higher density formation returns fewer emissions and *vice versa*.

The raw count-rates are stored in memory and then down-loaded at surface, after each bit run. The density data from each azimuthal bin can be processed to produce 360° depth calibrated false colour images of the borehole wall. By informal convention, relatively high density formation is assigned a bright false colour mapping, while low density formation is assigned a dark false colour mapping (Figure 4).

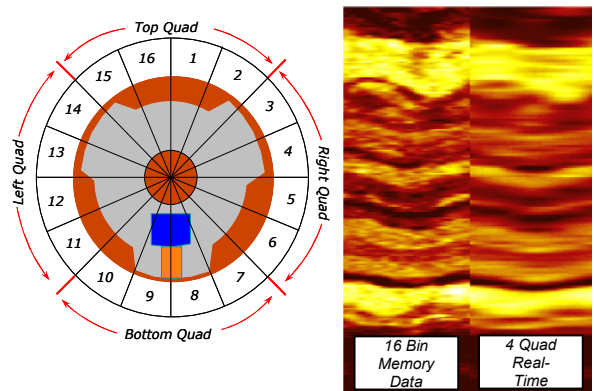


**Figure 4:** Diagram showing cross-section through the sectorised density measurements provided by the Sperry LWD Azimuthal Litho-density tool. Near right is an example of relatively high resolution sixteen sector recorded memory image. Far right is an example of four sector relatively low resolution real time image. Both the sixteen sector and four sector images represent 'unrolled' 360° images of the borehole wall. Inclined planar features which intersect the borehole appear as sine shaped bands of contrasting density. High density features have a bright false colour mapping while low density features have a dark false colour mapping.

The ALD tool can also produce real time (i.e. during drilling) images of the borehole wall. Limitations of mud pulse telemetry mean that real time density data can be assigned to only four azimuthal sectors, although an eight-sector assignment is now possible in the most recent generation of tools. Accordingly, real time images are (generally) of lower resolution than sixteen sector data. They are best used for identifying major variations in formation density such as those which may occur across fault cuts, fracture zones and sequence boundaries. The ALD tool also provides azimuthally binned photo-electric effect (PEF) measurements and an acoustic caliper to correct responses for stand off.

The tool contains conventional LWD sensors which were run during the logging of L13 and L13z. These included gamma ray, resistivity and neutron porosity

sensors. Detailed mud loss detection was also carried out during the drilling of L13 and L13z. PEF data were loaded into the L13 and L13z data base and processed to produce false colour images, but provided no additional detail.

An LWD imaging tool was used in the L13 and L13z in preference to a conventional post-drilling wireline conveyed imaging device because;

- The shallow depth of the Lennox reservoir, especially the shallow kick-off point from vertical, ensured that drill pipe conveyed logging would have been particularly time-consuming, requiring multiple wireline latches to log the long horizontal sections.
- During wireline logging of long horizontal sections, there is a risk of cable damage and differentially stuck tools.
- LWD real time images enabled decisions to be made during well steering with respect to completion planning during drilling.
- LWD imaging technology was deemed to be more time and cost efficient than drill pipe conveyed logging.

#### COMPLETION STRATEGY

After drilling, ECPs were made ready to run in the correct position on the completion strings. The aim was to isolate faults and fractures identified during real time logging. Where necessary, real time data were backed up by memory images down loaded at surface after each bit run. The real time images also confirmed the location of prognosed seismic scale fault cuts and allowed accurate determination of their down hole depths. Significant mud losses were recorded during the drilling of the L13 multilaterals. These ranged from < 10 bbl per hour to 110 bbl per hour and were used along with the images and the other LWD data (such as resistivity curves) to identify loss zones that were isolated via the ECPs. For the L13 lateral, five ECPs were set in total two 5 ½ inch predrilled scab liner intervals. For the L13z lateral, ten ECPs were set in total between four sections of pre-drilled scab liner.

#### MANUAL DIP PICKING

The sixteen sector memory ALD images were subject to a detailed post drilling structural interpretation. However, before manual picking of geological features could begin, the sixteen sector memory data was subject to quality control procedures based upon the guidelines of Loft *et al.*, (1997). There were three objectives;

- Ensure that features picked were located and orientated correctly.
- Identification of acquisition and drilling induced borehole wall aretefacts so that they may be distinguished from 'real' geological features.
- Determine the correct polarity of the image so that relatively high density features have a bright false colour mapping and relatively low density features have a dark false colour mapping.

The ALD image quality from L13 and L13z is good. Manual dips were picked directly from the ALD images using Terrasciences<sup>®</sup> software. Planar features crossing the well bore, such as a fracture or fault plane, appear as sine-shaped bands of varying density contrast when viewed on a 2D 'unrolled' display of the borehole wall (Figure 5). A sine-curve is interactively fitted over the geological feature to determine the orientation and dip magnitude.

#### MANUAL DIP PICKING VERSUS DIPMETER DATA

Manual dip picking has a number of advantages over conventional dip meter data.

- Actual geological features are picked. Automatically generated dipmeter dips are an average of several features over a specified depth interval.
- Manually picked dips are depth calibrated and can be assigned a geological category based on image log character, conventional (gamma, resistivity, neutron and density *etc.*) log responses and interpreter experience (*cf.* Table 2).
- Dipmeters cannot directly image or describe discordant (i.e. cross-cutting) relationships. Fracture characterization is therefore equivocal, relative to a manually picked image.
- Individual manually picked dips can be assigned a confidence rating ranging from 0 (very low confidence) to 1 (to high confidence). The resulting dip data set can therefore be filtered so that only high confidence dips are used for interpretation.

Individual manually picked dips from the L13 and L13z ALD images are typically assigned a high confidence rating. The manual dip classification scheme used for the Lennox ALD study is shown in Table 2.

Manual dip key	
Cross-stratified sandstone	
Dune bottom sets	
Stratified sandstone bedding	
Low density stratified sandstone bedding	
Stratified mottled sandstone bedding	
Oversteep / cross -bedding	
Mudstone bedding	
High density sandstone bedding	
Low density fracture	
High density fracture	

**Table 2:** Classification of manually picked geological features identified in the ALD images.

Eight of the feature types identified are of sedimentological significance. These were used to characterise depositional geometries and reservoir heterogeneities (Rizzi and Lean 2006). This aspect of the Lennox development plan is beyond the scope of this paper.

Dip orientations are referenced using the (informal) standard convention of dip/dip azimuth. For example, 10°/270° indicates a planar geological feature which has a dip of 10° towards 270° (referenced clockwise from north).

#### SCHMIDT STEREOONETS AND SPATIAL DATA

Stereoplots of planar data used in this paper are Schmidt upper hemisphere projections unless otherwise stated. Schmidt stereonet have the advantage that poles-to-planes plot in the quadrant in which they dip. For example, a plane dipping to the southwest has a pole that plots in the southwest quadrant of the stereoplot. This allows for ready visualization of spatial data distributions and is the informal industry standard for well bore derived orientation data (Figure 6).

#### STRUCTURAL INTERPRETATION

The objectives of the structural interpretation of the sixteen sector data are as follows;

- To confirm prognosed fault structures.
- To locate fractures.
- To account for significant drilling mud losses.

#### *Structural zonation*

Undeformed mudstone and heterolithic beds are considered reliable palaeohorizontal indicators and are typically used to determine structural dip; structural zones are identified as intervals of consistent or related palaeohorizontal bedding orientations. However, the

absence of mudstones and the scarcity of heterolithic bedding in both L13 and L13z, necessitated the inclusion of those sandstone beds considered to have been originally deposited at the horizontal in the structural zonations for the wells. While not ideal, this approach is permissible for two reasons:

- Horizontally stratified sandstone facies are a common occurrence within the Lennox Field Ormskirk Sandstone Formation and its onshore equivalent sheet-flood and aeolian sand-sheet facies (Macchi 2000; Meadows 2005).
- When plotted on Schmidt stereonet, sandstone bedding poles form a well defined cluster, indicating a mean orientation that is relatively consistent with that of heterolithic beds.

Nevertheless, because sandstone bed orientations may be influenced by sedimentological processes causing non-horizontal deposition, structural dips so derived should be regarded as lower confidence than if mudstone and heterolithic bedding features alone had been used. The term *dip domain* is used in preference to *structural zone* in such cases.

Wells L13 and L13z have been divided into three and four dip domains respectively. The dip domains and their possible structural significance with regards to fault identification and characterization are summarised in Tables 3 and 4.

#### *Fracture characterization*

Fractures were identified as bedding discordant features displaying continuity around the borehole circumference. The nature of the ALD tool image allows their classification as either high or low density relative to the host lithology (Figure 5). A total of 184 fractures were identified in L13, of which 105 were high density and 79 were low density. In L13z, 121 fractures were identified, composed of 28 high density and 93 low density features. High density fractures must be at least partially filled; low density fractures may be open or filled with low density materials and therefore have the potential to store or transport fluids.

Dip domain	Interval (ft MD)	Structural tilt and dip count	Comments
1	5875.2-6292.24	18°/275° (n = 71)	Beds dip consistently west.
2	A 6292.24-6494	14°/304° (n = 22)	Scatter of bedding dip azimuths about an overall W alignment; progressive increase in bed inclinations downhole.
	B 6494-7408	21°/281° 22°/280° (n = 135)	
	C 7408-7850	27°/299° (n = 27)	
	D 7850-8347.84	32°/261° (n = 36)	
3	8347.84-9064	15°/053° (n = 36)	Abrupt change to NE bedding dip azimuths at upper boundary.

**Table 3:** Dip domains identified during structural interpretation of L13. Red dashed lines represent fractured contacts or possible faulting.

Dip domain	Interval (ft MD)	Structural tilt and dip count	Comments
1	6420-7285.26	21°/283° (n = 115)	Dip domains represent relatively minor deviations from the overall moderate bedding dip towards WNW. Beds are consistently orientated within the domains.
2	7285.26-8270	16°/295° (n = 114)	
3	8270-8453.59	28°/289° (n = 15)	
4	8453.59-8677	16°/271° (n = 15)	

**Table 4:** Dip domains identified during structural interpretation of L13z. Red dashed line represents faulted contact.

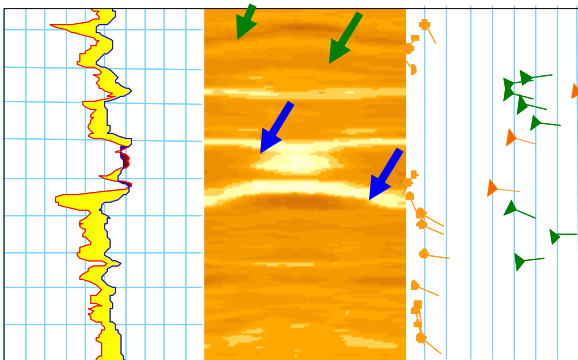


**Figure 5:** Examples of manually picked high density fractures which appear as bright sine shaped bands of high density (blue arrows) and are plotted as orange coloured triangular headed tadpoles in the far right column (vertical lines represent 10° divisions). Low density fractures appear as darker coloured bands (green arrows) and appear in the far right track as green coloured triangular headed tadpoles. Orange tadpoles are low angle (<10°) heterolithic beds. The far left track shows the neutron (blue) and density (red) curves. Note the increase in density adjacent to the high density fractures. Lateral well L13z.

As would be expected in closely spaced wells, fracture orientations are relatively consistent across both well paths, displaying a strong north-south strike bias. This north-south fracture strike is itself consistent with the strike of regional faults. Dip inclinations are more variable, with a slight bias towards easterly dip directions in L13 emphasized in L13z (Figure 6).

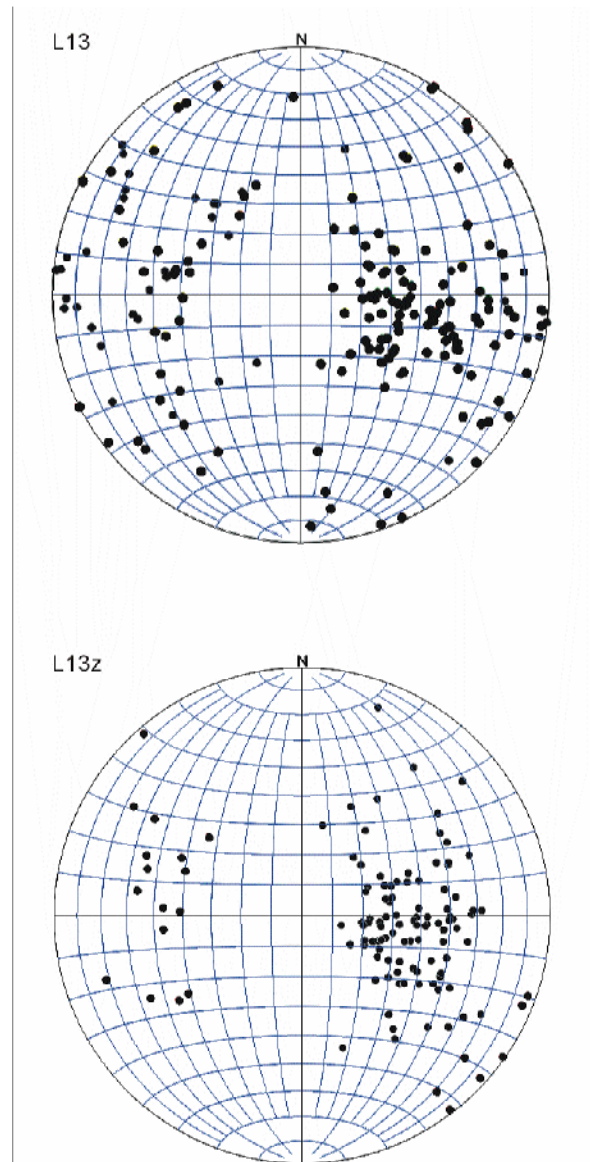


**Figure 6:** Upper hemisphere Schmidt stereonet of poles to fracture planes for wells L13 and L13z. The poles (black dots) dip toward the east and west suggesting fracture planes are aligned north-south.

Orientated data derived from any well are subject to a geometrical bias, in that those features lying parallel or near-parallel to the well path are under sampled with respect to those orientated perpendicular to the well bore. The fracture counts for both L13 and L13z are

therefore likely to represent an under-determination of the true (three dimensional) fracture frequency in the surrounding rockmass. The wider scatter of fracture azimuths in L13 compared to L13z may illustrate this *borehole bias* effect: L13z is aligned east-west whereas the L13 well path swings through almost 90° from east to north-northeast and is therefore likely to intersect a wider range of feature orientations (Figure 7). Statistical correction for the borehole bias effect according to Terzaghi, (1965) yields corrected counts of 529 fractures in L13 and 241 in L13z.

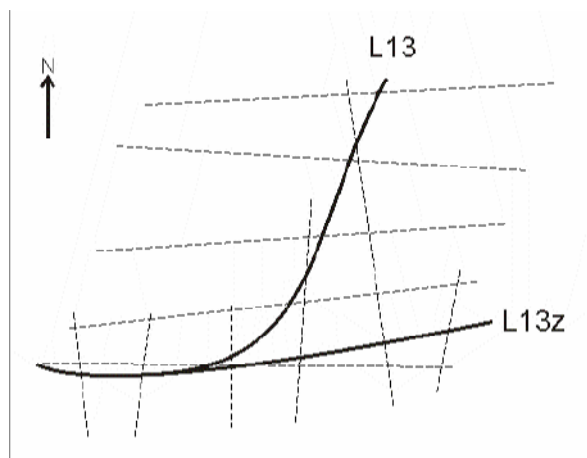


**Figure 7:** Schematic plan view sketch map of well paths (solid) demonstrating how, while both L13 and L13z would intersect most N-S striking fractures (dashed lines), L13 would intersect a higher proportion of E-W striking fractures in the region than L13z due to borehole bias. L13z well path *circa* 1 km.

#### Fault characterization

Several candidate fault intersection depths were supplied in the end-of-well report: at 6348 ft (Fault D) and 7040 ft (Fault A) in L13 and at 7181 ft (Fault A) and 8270 ft (Fault B) in L13z. Of these, only Fault A was prognosed to intersect both L13 and L13z. Mud losses from L13z support the placement of Fault A at 7181 ft, but no proxy indicators of faulting (e.g. mud loss, fault drag or fracturing) were apparent at 7040 ft in L13. A cluster of manually picked high density fractures at 7017 ft in L13 suggests that Fault A may have been incorrectly identified during drilling (Figure 8). In either case, if Fault A is indeed a continuous structure, its intersection with the two wellbores requires that it cross-cuts the strong N-S background fracture strike, unless it is itself displaced along a non-imaged fault lying between the wells. Fault B was prognosed to intersect L13z at 8270 ft. Manual dip picking identified a fracture zone extending 8230-8315 ft, which may represent a fault damage zone. Fault D was prognosed to occur at 6348 ft in L13. This is on-depth with a fault inferred from progressive bedding rotation (possible fault drag) identified from the manually picked dataset (Figure 9).

Manually picked bedding drag patterns indicate that in addition to the Faults A and D, the L13 well path may intersect a further four faults, whose displacement surfaces are below the resolution of the ALD image. These candidate faults (6070 ft, 6885 ft, 7190 ft and 8488 ft) were identified from bedding dip rotations that may indicate drag. No additional faults were confidently inferred in L13z.

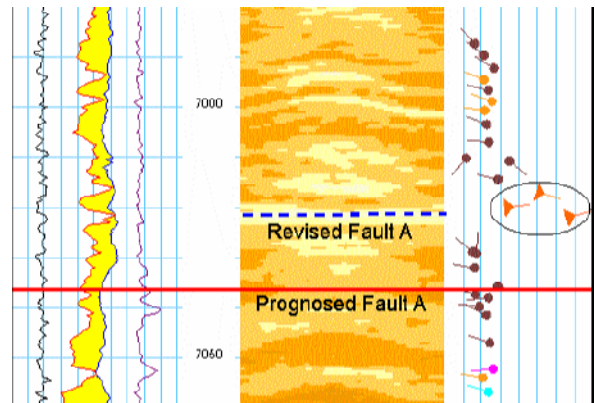


**Figure 8:** Prognosed position of Fault A (red line) and suggested revised position of Fault A (blue dashed line), based on the occurrence of a high density fracture cluster at 7017 m. These fractures appear as orange coloured triangles in the right hand dip track. Far left track shows porosity (blue) and density (red) curves. Brown tadpoles = sandstone bedding, orange tadpoles = heterolithic beds, pink tadpoles = bed base, pale blue tadpoles = cemented bed.

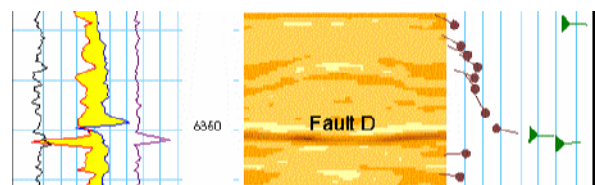


**Figure 9.** Candidate fault drag seen as increase in dip approaching 6348 ft MD of Fault D in L13 with dip reversal of bedding below. Although discontinuities are apparent at the culmination of the rotation, they are classed as fractures rather than a fault since no offset of bedding is apparent. Confidence of fault occurrence at this depth is nevertheless high, and the 'fractures' may represent the fault plane itself or reflect its orientation.

#### Fracture distribution and mud losses

Drilling mud losses recorded in the end-of-well report were compared with manually picked features in an attempt to ascertain their cause(s). Most losses coincide with manually picked fractures, but given the relatively common occurrence of fractures in the images, this relationship could be considered equivocal. In addition to any obviously spatially associated structures, it must be noted that mud losses can also be time-dependent, and/or related to events not local to the borehole. This increases the complexity of relationships between losses and geological features to a degree where only very strong direct associations can be

regarded as unequivocal; losses at any given depth may also result from a combination of factors. Nevertheless, the association of imaged fractures with many mud losses may indicate that some fractures are at least partially open, with apertures sufficient to act as conduits for drilling mud. Of particular note, however, is the coincidence of two of the largest losses in L13 with inferred faults: 100 bbl/hr at 6350 ft and 110 bbl/hr at 6887 ft. Fault D was reported at 6350 ft, but no structure was prognosed at 6887 ft prior to image analysis. Fracture and fault apertures could not be determined from the ALD data, but were clearly large enough to allow significant mud escape.

Losses of similar scales were not recorded in L13z; the highest escape rate of 40 bbl/hr coincides with Fault A, but the fault was likely identified by this mud loss and no evidence of faulting was identified from the images. Well L13z may therefore represent a case in which some open fractures are present, but which are below the resolution of the ALD tool. It may also be that imaged fractures are absent from these intervals because fractures were enhanced or became open (with time) after passage or withdrawal of the LWD assembly. Such drilling-enhanced fractures are by no means uncommon; in this situation fractures must occur at shallower depths (MD) than the mud losses suggest.

Disregarding the dip component of fracture orientations, a strong association between mud losses and north-south striking fractures is apparent in both wells. It is likely to be heavily influenced by borehole bias in L13z, but also holds true in L13, which swings from an east-west to a north-south azimuth. The association between mud losses and N-S fracture strike may therefore be regarded as having a moderate confidence.

**IMPLICATIONS FOR RESERVOIR QUALITY**

The identification of sub-seismic scale fractures and faults, and confirmation of prognosed seismic scale faults has a number of implications for reservoir characterization. Faulting may have been on such a scale to have generated clay smears, which would act, at least in part, as potential barriers to fluid flow. Fractures are typically steeply dipping, suggesting they may act as baffles to lateral fluid flow. This would be particularly true for high density fractures, whose character reflects fracture fill by cementation, or maceration of sand grains along granulation seams. Such granulation seams are often preferentially cemented and are a common feature of onshore United Kingdom Triassic outcrops where they typically stand proud from weathered outcrops. Fractures are not randomly distributed along the L13 and L13z well

paths. They typically occur as clusters located at reservoir zone contacts. Fractures also occur within reservoir zones as isolated features and clusters. Lateral fluid flow between and within reservoir zones may therefore be hindered.

**WELL RESULTS**

The L13 and L13z well results have been recently discussed by Clarke *et al.* (2006). The multilaterals commenced production in August 2005 at an initial rate of 7000 to 8000 bopd. The well has produced 40% more than its predicted oil volume to the end of February 2007 (Figure 10). However, production performance has been unusual. The initial high rates of production declined quickly as the GOR of the well increased. As deduced from the structural interpretation, and mud losses, it is possible that some fractures are below the resolution of the ALD imaging sensor, and thus were not isolated by ECPs and black pipe. These fractures could be acting as a conduit for gas from the gas cap to enter the well bores. L13 and L13z are now produced intermittently to prevent gas from choking production from the oil rim. Recent optimization of production has improved average L13 oil rates.

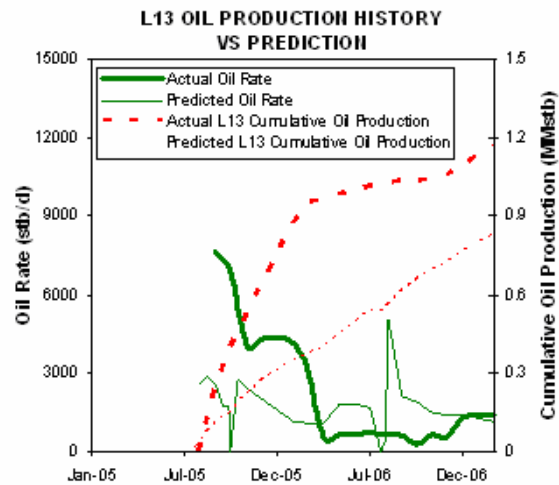


Figure 10: L13 actual oil rate and cumulative oil production compared with predicted oil rate and cumulative production.

**SUMMARY AND CONCLUSIONS**

1. Although the ALD imaging tool is relatively low resolution compared to more conventional imaging tools, high quality dip data can be extracted using a sound knowledge of structural geology and borehole geometric relationships.
2. Structural analysis of the L13 and L13z manual dip data set has enabled division of both study intervals to be divided into dip domains of near

- consistent azimuth and dip magnitude. Three dip domains have been identified in L13 and four dip domains have been identified in L13z.
3. Due to the paucity of mudstone beds and other indicators of the palaeohorizontal, structural tilt was determined using near horizontally stratified sandstones.
  4. Fractures have been identified as being relatively high density or low density relative to adjacent formation.
  5. A total of 184 fractures have been identified in sidetrack L13, 121 fractures in sidetrack L13z. Statistical analysis suggests that the number of fractures picked is significantly undersampled.
  6. Borehole bias is demonstrated by a north-south fracture strike in L13z which has a near east-west orientated well section. Compare this with a much wider range of fracture strikes in L13, which rotates 90° anticlockwise.
  7. Fractures typically occur in clusters, some of which are coincident with dip domain and reservoir zone boundaries.
  8. Fracture-associated bedding drag dip patterns suggest that in addition to prognosed seismic scale faults cuts, there may be up four other additional sub-seismic scale faults in L13.
  9. A fracture cluster suggests that Fault A may be encountered at 7017 ft in L13 rather than 7040 ft. The strike of Fault A may cut across the north-south tectonic fabric, or may be offset by another fault which has not been identified.
  10. A relationship between drilling mud losses and north-south fracture strikes exists in both the L13 and L13z laterals. This relationship would have been attributed to borehole bias, were it not for the 90° anticlockwise rotation of the L13 well path.
  11. Drilling mud seepages within intervals that contain no visible fractures may suggest that some open, or at least partially open fractures are present that are below the resolution of the ALD imaging sensor. It may also be possible that some fractures became open after passage of the LWD sensor.
  12. No *in situ* stress indicators were observed in either the L13 or the L13Z lateral.
  13. Initial high oil rates declined quickly as the GOR of the well increased. This supports the view that some fractures were below the resolution of the logging tool and were thus not isolated, allowing gas from the gas cap to enter the well bores.
  14. Detailed structural analysis of the L13 and L13z well bores and the well results has significantly improved the understanding of the Lennox Field and other EISB assets.

#### ACKNOWLEDGEMENTS

The management of BHP Billiton Petroleum Pty Ltd and the Joint Venture partners for Lennox, ENI UK Limited, are thanked for permission to publish this paper. In addition the authors would like to thank the following BHP Billiton staff for their significant input to the project: the London Drilling Department, Tony Cave, Spencer Quam, Andy Edgar, Jim Ayton, James Ryan, Simon Barnes, Neil Hopkins and Stewart Brotherton. Giancarlo Rizzi and Brian Callaghan would like to thank Adam Styles for supervising the structural interpretation and all at Task Geoscience for their support during the preparation of this paper, particularly Stuart Buck, Roddy M<sup>c</sup>Garva and Lawrence Bourke.

#### REFERENCES

- Clarke, A. *et al.*: "Case Study: Lennox – The Race to Produce Oil Prior to Gas Cap Blowdown", paper SPE 100126 presented at the 2006 SPE/EAGE European Annual Conference, Vienna, Austria, 12-15 June.
- Jackson, D.I. and Johnson, H. 1996. *Lithostratigraphic nomenclature of the Triassic, Permian and Carboniferous of the UK offshore East Irish Sea Basin*. British Geological Survey Nottingham.
- Jackson, D.I. and Mullholland, P. 1993. Tectonic and stratigraphic aspects of the East Irish Sea Basin and adjacent areas; contrast in their post-Carboniferous structural styles. In: Parker, J.R. (ed.) *Petroleum Geology of Northwest Europe: proceedings of the 4<sup>th</sup> Conference*. Geological Society, London, p.791-808.
- Lofts, J.C., Bedford, J., Boulton, H., Van Doorn, J.A., and Jeffreys, P. 1997. Feature recognition and the interpretation of images from horizontal wellbores. In: Lovell, M. A. & Harvey, P. K. (eds.) *Developments in Petrophysics*, Geological Society Special Publication, 122, p.345-365.
- Macchi, L. 2000. A review of facies distributions in the Lennox Field. *Unpublished internal report for BHP Billiton Limited*. pp.22.
- Meadows, N.S. 2006. The correlation and sequence architecture of the Ormskirk Sandstone Formation in the Triassic Sherwood Sandstone Group of the East Irish Sea basin, NW England. *Geological Journal*, 41, p.92-122.
- Meadows, N.S. 2005. *Excursion guide to the margins of the East Irish Sea and Cheshire Basin*. Proprietary guide for BHP Billiton Limited. ISBN 1 901901 40 8, pp.44.
- Meadows, N.S. and Beach A. 1993. Structural and climatic controls on facies distribution in a mixed fluvial and Aeolian reservoir; the Triassic Sherwood Sandstone in the Irish Sea. In: North C. P., Prosser, D. J. (eds.), *Characterization of fluvial and aeolian reservoirs*, Geological Society of Special Publication No. 73, p.247-264.
- Rizzi, G. and Lean, J. 2006. Sedimentological interpretation of Azimuthal Lithodensity images, Lennox Field, Block

110/15a, UKCS. British Sedimentological research Group Abstracts. University of Aberdeen, United Kingdom.

Terzaghi, R.D. 1965. Sources of error in joint surveys. *Geotechnique*, 15, p.287-304.

Thompson, J. and Meadows, N.S. 1997. Clastic sabkhas and diachroneity at the top of the Sherwood Sandstone Group: East Irish Sea Basin. In: *Petroleum geology of the Irish Sea and Adjacent Areas*. Meadows, N. S., Trueblood, S. P., Hardman, M. and Cowan, G. (Eds.). Geological Society Special Publication No.124, pp.237-252.

Warrington, G., Wilson, A.A., Jones, N.S., Young, S.R. and Haslam, W.W. 1999. Stratigraphy and sedimentology. In: Plant, J.A. Jones, D.G. and Haslam, H.W. (eds.) *The Cheshire Basin: Evolution, fluid movement and mineral resources in a Perm-Triassic rift setting*. British Geological Survey, Keyworth. Nottingham, p.10-40.

Yaliz, A., Chapman, T. and Downie, J. 2002. Case study of a quad-lateral horizontal well in the Lennox Field: A Triassic oil-rim reservoir. *Society of Petroleum Engineers. SPE publication 75249*. SPE/DOE Improved Oil Recovery Symposium, Tulsa, Oklahoma, 13-17 April.

Yaliz, A., and Chapman, T. 2003. The Lennox oil and gas field, Block 110/15a, East Irish Sea. In: Gluyas, J. G. and Hitches, H.H. (eds.), *United Kingdom oil and gas fields commemorative volume*. Geological Society, London, Memoir 20, p.87-96.

#### ABOUT THE AUTHORS

Giancarlo Rizzi is a sedimentologist with Task Geoscience Ltd, Aberdeen UK where he is responsible for the sedimentological interpretation of bore hole images and other down hole data. Giancarlo holds a degree in Geology from the University of London and a Ph.D. from the University of Glasgow. He has ten years experience within the oil industry. International assignments have included Azerbaijan, Venezuela, Nigeria, Malaysia, Guyana and Libya. He has published several scientific papers in international journals and is a former Aberdeen Director and Director of Education for the Petroleum Exploration Society of Great Britain (PESGB). He was the lead convener of two recent international conferences. Currently he is studying for a Diploma in mathematics.

Brian Callaghan is a structural geologist who has worked at Task Geoscience in Aberdeen, Scotland since 2005. His role includes determination of structural tilt over logged intervals, the analysis of curvature and discontinuity data and the resolution of *in-situ* stress component directions. Brian studied geology at University College Cork (Ireland) before gaining a Ph.D. from the National University of Ireland, Galway,

and is a published author. He entered the hydrocarbon exploration industry in 2001 and has worked in the United States, Africa and Europe on projects from around the world.

Jonathan Lean is a Petrophysical Advisor now with Hess Ltd in London where he provides petrophysical and formation evaluation support for his employers exploration and production activities in the UK, Norway and Denmark. He has previously been employed by Enterprise Oil in Aberdeen, Scotland, by PGS Reservoir Consultants in Maidenhead, England and by BHPBilliton Petroleum in London. He holds a MEng degree in Petroleum Engineering from Imperial College, London and is an Associate of the Royal School of Mines. He is a member of the Society of Petroleum Engineers and serves on the Board of the London Petrophysical Society, the London Chapter of the Society of Petrophysicists and Well Log Analysts (SPWLA).

David Lawton is currently Geological Advisor for activities in North-West Europe for Hess Limited in London, following over 20 years industry experience for companies including BHPBilliton, Amoco and Fina. He holds a B.Sc (Hons) in Geology from Plymouth Polytechnic and an M.Sc in Sedimentology from the University of London. His experience has been focused on development and appraisal projects, with specific experience working on fluvial/aeolian reservoirs in the Southern North Sea, the East Irish Sea and North Africa. He is a member of The Geological Society, the Petroleum Exploration Society of Great Britain (PESGB), the London Petrophysical Society (LPS) and the AAPG.

Alison Clarke is a Senior Reservoir Engineer with BHPBilliton Petroleum, London UK. She is responsible for providing reservoir engineering input to support production activities at the Liverpool Bay asset in the East Irish Sea. Alison holds a B.Eng (Hons) degree in Petroleum Engineering from the University of NSW, Sydney. She has 11 years experience in the oil industry and has previously been employed by Santos in Brisbane, Australia. Alison is a member of the Society of Petroleum Engineers.

Tim Parker is a Principal Log Analyst working for Halliburton in Aberdeen, UK. His primary focus is on LWD services for Sperry Drilling Services, supporting the UK, Western Europe and Russia. He holds a degree in Physics from the University of Bristol and an MBA from Warwick Business School. Tim has worked in the industry for over 17 years, the last 12 of which have been with Sperry, in which time he has held positions in field operations, operations management and

petrophysics. Previously he worked in the UK and internationally as a wireline field engineer. He is a current committee member of the Aberdeen Formation Evaluation Society (AFES).